Published in final edited form as:

Cytometry A. 2018 July ; 93(9): 894–904. doi:10.1002/cyto.a.23574.

Proteomic profiling of native unpassaged and culture-expanded mesenchymal stromal cells (MSC)

Erika Moravcikova[1], **E. Michael Meyer**[2], **Mirko Corselli**[3], **Vera S. Donnenberg**[1,2,4,#], and **Albert D. Donnenberg**[2,4,5,#]

[1]University of Pittsburgh School of Medicine, Department of Cardiothoracic Surgery, Pittsburgh, PA

[2]University of Pittsburgh Cancer Institute, Pittsburgh, PA

[3]BD Biosciences, La Jolla, CA

[4]McGowan Institute of Regenerative Medicine, Pittsburgh, PA

[5]University of Pittsburgh School of Medicine, Department of Medicine, Pittsburgh, PA

[#]these authors share senior authorship

Abstract

Human culture-expanded mesenchymal stromal cells (MSC) are being considered for multiple therapeutic applications because of their regenerative and anti-inflammatory properties. Although a large number of MSC can be propagated from a small initial sample, several lines of evidence indicate that MSC lose their immunosuppressive and regenerative potency after multiple passages. In this report we use the FACSCAP Lyoplate proteomic analysis system to detect changes in cell surface protein expression of CD45−/CD31−/CD34−/CD73+/CD105+ stromal cells in unpassaged bone marrow and through 10 serial culture passages. We provide for the first time a detailed characterization of native unpassaged bone marrow MSC (0.08% of bone marrow mononuclear cells) as well as the changes that occur during the initial expansion. Adipogenic and osteogenic differentiative potential was determined though the serial passages and correlated with immunophenotypic changes and senescence. Among the most prominent were striking decreases in Fas ligand, CD98, CD205 and CD106, accompanied by a gain in the expression of CD49c, CD63, CD98, and class 1 and class 2 major histocompatibility complex (MHC) molecules. Other molecules that are down-modulated with later passage include CD24, CD54, CD59, CD243/P-glycoprotein, and CD273/PD-L2. Early senescence, as defined by loss of replicative capacity occurring with loss of differentiative capacity, increase in *CDKN2A p16* and increased time to confluence, was accompanied by loss of the motility-associated metalloproteinase CD10 and the proliferation-associated transferrin receptor CD71. Among the strongest statistical associations

Corresponding authors: Vera S. Donnenberg, PhD, F.C.P., Associate Professor of Cardiothoracic Surgery, 5117 Centre Avenue, Suite 2.42, 15213 Pittsburgh, PA, USA, donnenbergvs@upmc.edu, Phone: (412) 623-3256, Albert D. Donnenberg, Ph.D., Professor of Medicine, 15213 Pittsburgh, PA, USA, donnenbergad@upmc.edu, Phone: (412) 623-3256.

Author Contributions. Erika Moravcikova, Vera Donnenberg and Albert Donnenberg designed the experiments and analyzed the data. E. Michael Meyer operated the flow cytometer and contributed to panel design. Mirko Corselli contributed to panel design. Albert Donnenberg and Erika Moravcikova wrote the manuscript. Erika Moravcikova is a fellow in the Donnenberg Laboratory and performed all the experiments in this manuscript.

Conflict of interest: The authors have no conflicts of interest to disclose. MK is an employee of BD Biosciences

were loss of MAC-inhibitory protein/CD59, loss of ICAM-1/CD54, and increase in *CDKN2A* as a function of increasing passage, as well as increased CD10 expression with adipogenic and osteogenic capacity. The data provide clear set of markers that can be used to assess MSC quality. We suggest that clinically relevant numbers of highly functional low passage MSC can be manufactured starting with large quantities of bone marrow, which are readily available from cadaveric organ donors.

Keywords

Mesenchymal stromal cells (MSC); proteomic; CD73; CD105; Lyoplate; osteogenesis; adipogenesis; bone marrow; unpassaged bone marrow MSC

Introduction

Human bone marrow derived mesenchymal stem cells (BM MSC) are multipotent cells with a high capacity for self-renewal (1). Although autologous MSC retain the ability to differentiating into adipose, bone and cartilage, by far the most prevalent clinical applications have been anti-inflammatory therapy and promotion of wound healing (2). Unlike regenerative applications, anti-inflammatory therapy does not require autologous cells and is amenable to production of a standardized cryopreserved cellular product maintained as a cell bank of low passage cells and expanded subcultures (3). One impediment to the manufacture of optimal cellular products is the lack of biomarkers associated with MSC function. This is compounded by the fact that, *in vivo*, BM MSC are a rare population and therefore native MSC have been relatively poorly characterized.

In vivo animal models of autoimmunity have been used to evaluate the anti-inflammatory properties of human MSC, and improvement in symptoms has been noted after system administration in models of acute lung inflammation(4), inflammatory bowel disease, multiple sclerosis, diabetes, myocardial infarction, cerebral vascular disease, inflammatory lung disease and graft versus host disease (GVHD) (reviewed in (5)). Cultured MSC appear to counterbalance the effects of pro-inflammatory macrophages which have been activated by sterile tissue damage or infectious agents. Inflammatory macrophages produce IL-1α, IL-1β and TNF-α, which in addition to their proinflammatory effects also activate the immunosuppressive effects of MSC, influencing local macrophage polarization and dampening the downstream effects of proinflammatory cytokines(6). In particular, PGE2 secreted by activated MSC induces tissue macrophages to secrete the potent anti-inflammatory cytokine IL-10, which in turn inhibits macrophage release of pro-inflammatory cytokines TNF-α, IL-6 (7). MSC, and particularly their adipose-derived counterparts, can also directly inhibit differentiation of dendritic cells (8), down-modulating T-cell costimulatory molecules and inhibiting Th1 polarization (9). Numerous clinical trials have been conducted in disease conditions including cardiovascular, respiratory, neurological, traumatic, congenital, orthopedic, neoplastic and autoimmune (10–12).

MSC lack endothelial and hematopoietic markers (CD31, CD34, CD45, Glycophorin A) but express cell surface markers CD73, CD105, CD90 (13). While no single molecule of mesenchymal stemness has been identified, we have evaluated the cell surface proteomic

changes of expanded MSC from unpassaged up to passage 10, and have identified a pattern of cell-surface protein expression associated with cell death, immune regulation, transport, adhesion, motility and proliferation, which uniquely characterize unpassaged and low-passage MSC and correlate with the ability to proliferate and differentiate into osteogenic and adipogenic lineages.

Material and Methods

Isolation and expansion of bone marrow mesenchymal stem cells and foreskin fibroblasts

Mesenchymal stem cells were isolated from vertebral bone marrow from a cadaveric organ donor. Approval for retrieval of vertebrae from braindead organ donors was granted by the Center of Organ Recovery and Education (CORE), the local organ procurement organization, and the University of Pittsburgh Committee for Oversight on Research Involving the Dead (CORID). Bone marrow mononuclear cells were isolated from vertebral bodies as previously described (14). Briefly, crushed vertebrae were irrigated with medium containing normal saline, albumin (0.5 g/dL), DNAse (350 U/mL; Pulmozyme, Genentech, San Franciso, CA, USA), $MgCl_2$ (2.5 mM), sodium heparin (10 U/mL) and gentamicin (50 μg/mL), and crushed in Biorep bone grinder (Biorep Technology, Miami, FL). The crushed bone was strained serially through stainless steel sieves (W. S. Tyler, St Catharines, ON, USA; 425 μm, 180 μ m) and the strained cell-rich filtrate pooled and filtered (500 μm, 200 μm) using a BM collection filter set (4R-21–07; Baxter, Deerfield, IL, USA). The filtered product was centrifuged at 700 × g and cryopreserved in cryoprotectant containing 0.9% saline, 10% DMSO (OriGen Biomedical, CP-50) and 5% human serum albumin (Baxter, 060048).

One vial of cryopreserved bone marrow nucleated cells containing 50×10^6 cells before cryopreservation was seeded in a 150 cm^2 flask and cultured in MEM (45000–382, Corning, NY, USA) supplemented with 10% fetal bovine serum (FBS, S11550, Atlanta Biologicals, Flowery Branch, GA, USA) 100 U/mL penicillin G (P3032, Sigma-Aldrich), 50μg/mL gentamicin (G1264, Sigma-Aldrich) in 37 °C, 5% CO_2 incubator (Heracell, ThermoFisher Scientific). After 24 h, non-adhered cells were removed by media replacement. Adherent stromal cells were split 1:5 when they reached 80% confluency, up to passage 10. The culture time-line and seeding density are shown in Figure S1. A portion of the cells from each passage was cryopreserved for subsequent studies.

Primary human foreskin fibroblasts (AVDHFF-1, 2 and 3) were cultured from anonymized medical waste material using standard methods (15), and were propagated in DMEM high glucose (Cat. No. 11965, Invitrogen), 15% fetal bovine serum (HyClone, GE Healthcare Life Sciences), 100U/mL penicillin G (Cat. No. P3032, Sigma), 50μg/mL gentamicin (Cat. No. G1264, Sigma), 2 mM L-glutamine, 10 mM HEPES buffer (Cat. No. H4035, Sigma), and 5×10^{-5} M 2-mercaptoethanol (Cat. No. M6250, Aldrich).

Adipogenic and osteogenic differentiation of mesenchymal stem cells

The cryopreserved cells (1 mL, ~ 2×10^6 cells) were rapidly thawed at 37˚C and 9 mL of ice cold MEM supplemented with 10% of FBS, 100 U/mL of penicillin G and 50μg/mL of

gentamicin, was slowly added. Cells were counted using a ViCell imaging cell counter (Beckman Coulter) and 50,000 cells from passage 2, 3, 5, 7 and 10 were seeded in 24-well plates in MEM supplemented with 10% of FBS, 100 U/mL of penicillin G and 50μg/mL of gentamicin. After 24-hours, medium was replaced with medium containing 0.1% ethanol (control) or adipogenic medium (MEM, 10 % of FCS, 100 U/mL of penicillin G, 50 μg/mL of gentamicin, 1μM of dexamethasone (D4902, Sigma-Aldrich), 0.5 μM 3-Isobutyl-1-methylxanthine (I5879, Sigma-Aldrich), 60μM of indomethacin (I7378, Sigma-Aldrich), and 10 μg/ml insulin (I5500, Sigma-Aldrich)) or osteogenic medium (MEM, 10 % of FCS, 100 U/mL of penicillin G, 50 μg/mL of gentamicin, 0.1μM dexamethasone, 50μg/mL of L-ascorbic acid-2-phosphate (A8960, Sigma-Aldrich), 10mM of beta-glycerolphosphate (G9891, Sigma-Aldrich). Cultures from all passages were plated on the same day. Medium was replaced every three days. After 21 days, cells were fixed with 2% methanol-free formaldehyde (04018–1, Polysciences, Warrington, PA, USA) for 20 min at RT. For adipocyte visualization, cells were washed with 60% of isopropanol and 0.4 % (weight/volume) of oil red O was added for 10 min. Cells were washed 4 times with ddH_2O. For osteocytes visualization, fixed cells were washed twice in PBS, and incubated with 1.4% of Alizarin Red (A-5533, Sigma), pH 4.2, for 10 min at RT. Subsequently, cells were washed 4 times with ddH_2O. Photomicrographs were taken with Zeiss microscope equipped with AxioVision 482 software. Uniform LUT settings were used for all images. Osteogenic differentiation was quantified using a solution of 20% methanol and 10% acetic acid in water. After 15 minutes, liquid was transferred to a 96-well plate and the quantity of Alizarin Red was determined on the Vmax kinetic microplate reader (PM269746, Molecular Devices, San Jose, CA) at a wavelength of 490nm. Adipogenesis was quantified by counting the cells with at least five large oil red vesicles in five fields of low-power objective (x20) and normalized to total cells in the field.

Isolation of RNA and RT-qPCR

Cells (0.6×10^6) were seeded in 24-well plates. Cells were differentiated for 7 days and then lysed directly into RNA lysis buffer containing 14 mM β-mercaptoethanol. Total RNA was isolated using the RNeasy Plus Micro kit (74034, Qiagen) according to the manufacturer's instructions. RNA was reverse-transcribed to cDNA using the cDNA Affinity Script Kit according the manufacturer's instructions (600559, Agilent Technologies, Santa Clara, CA). The primers for *PPARG, RUNX2* were designed using the PrimerQuest Tool (Integrated DNA Technologies, Coralville, IA) and *ACTB* primers were designed using the program Primer Express (Applied Biosystems, Foster City, CA; Supporting Information Table S1). The 20 μl of RT-PCR reaction mixture contained Sybr Green Master Mix (Cat No. 04913914001, Roche, Basel, Switzerland), 200 nM of the primers, and 0.5 μl of cDNA. Real-time RT-PCR was run in duplicate in semi-skirted 96-well PCR reaction plates (401334, Agilent Technologies) on the Stratagene Mx3005P instrument (Agilent Technologies). The PCR amplification included a hot start at 95°C for 15 min, 40 cycles of denaturation at 95°C for 15 s, annealing at 60°C for 20 s, and extension at 72°C for 20 s. The threshold cycle (C_τ) values of the amplification reactions were determined with the Mx3005P system software (Agilent Technologies). Data were normalized to *ACTB* and expressed as linearized C_τ (*i.e.* $2^{-\Delta C\tau}$).

Flow cytometry for classical mesenchymal markers

Freshly frozen and expanded bone marrow (BM) cells as well as cultured human foreskin fibroblasts AVDHFF cells were washed with ice cold immunofluorescence assay buffer (IFA, 4% calf serum, 2 mM EDTA in PBS without Ca^{2+} and Mg^{2+}, pH 7.2) and the viability was assessed by Trypan Blue staining using hemocytometer. Cells were blocked with mouse serum for 20 min at 4°C. Cells were divided to be stained for 20 min at 4°C with a panel consisting of CD31-APC (R &D Systems, Cat. No. FAB3567A), CD45-APCCy7 (BD Cat. No. 348805), CD73-PE (BD Cat. No. 550257), CD34 ECD (Beckman Coulter Cat. No. IM2709U), CD90-PECy5 (Beckman Coulter Cat. No. IM3703), CD105-FITC (Fitzgerald Cat. No. 61R-CD105DHUFT), CD4-BV785 (BioLegend Cat. No. 317442). Cell were washed with IFA, fixed with 2% paraformaldehyde for 20 min at RT and permeabilized with 0.05% Saponin for 10 min at RT. Cells were washed with IFA and incubated with RNAse A for 10 min at 37C. Finally, DAPI was added to the cells at a concentration of 8 μg/ml and cells were acquired on Fortessa flow cytometer (BD Biosciences). The instrument was set up using CS and T beads (BD Biosciences) and PMT voltages were adjusted to predetermined target channels using the 7^{th} peak of 8-peak Rainbow Calibration Particles (Spherotech, Lake Forest IL, RCP-30–5A) as a reference point. FITC, APC and PE Calibrite beads (BD Biosciences), single stained antibody capture beads (tandem fluorochromes, BD Biosciences), and unstained cells (DAPI) were used as spectral compensation standards. Acquired data were analyzed using VenturiOne Software (Applied Cytometry Systems) and clusters were generated in SysStat Software (San Jose, CA, USA).

Multicolor-flow cytometry-based cell surface profiling

Freshly cryopreserved bone marrow (BM) cells and cultured mesenchymal cells were thawed in 50% bovine serum. BM cells were treated with DNAse (0.15 mg/ml, Dornase alfa, Genentech Inc., San Francisco, CA) and mononuclear cells were isolated using density gradient centrifugation (10771, Histopaque®−1077, Sigma-Aldrich). Mononuclear cells from BM and cultured MSCs were washed twice with ice cold and the viability was assessed by Trypan blue staining using a hemocytometer. Non-specific binding sites and Fc receptors were blocked with mouse serum for 20 min and cells were then divided in equal parts for FMO and DAPI only controls. Unpassaged BM cells and passaged MSC were first stained in bulk with a backbone panel, using different panels for unpassaged and passaged cells. The backbone panel for unpassaged BM consisted of: CD14-BUV737 BD Cat# 564444, CD105-BUV395 BD Cat# 563803, CD34-BV786 BD Cat# 744741, CD73PECy7 BD Cat#561258, CD235aPECy5 BD Cat# 559944, CD45APCR700 BD Cat# 566041. The backbone panel for cultured MSC, which were documented to be CD73+/CD105+ (Figure 1), was: CD90 biotin BD Cat# 555594 plus streptavidin ECD Beckman Coulter Cat# IM99512, CD45-PE-Cy5.5 Invitrogen Cat# MHCD4518, CD31 PE-Cy7 BD Cat# 563651, CD34-A700 BD Cat# 561440 and CD146-BV711 BD Cat# 563186. Bulk-stained cells were then divided to a 96-well plate containing FITC, PE and APC-conjugated antibodies specific to 228 cell proteins (BP80394, BDT FACSCAP Lyoplate, BD Biosciences, San Diego, CA, USA). Plates were incubated in the dark and centrifuged at 240 g for 7 min. Cells were fixed with 2% methanol-free formaldehyde for 20 min, permeabilized with 0.05% Saponin in IFA buffer consisting of 4% calf serum, 2 mM EDTA in PBS without Ca^{+2} and Mg^{+2} (pH 7.2) and washed with IFA buffer. Finally, DAPI (Invitrogen, Cat. No. D1306) was added to the cells

at a concentration of 8 μg/ml and plates were acquired on Fortessa SORP flow cytometer (BD Biosciences) equipped as described in MIFlowCyt. Instrument setup, spectral compensation and data analysis were performed as described above.

Statistical Analysis.

Statistical analysis, including Student's t-test and Pearson correlation, was performed using SYSTAT Version No. 13.00.05 (Systat Software, San Jose CA). P-values associated with Pearson's coefficient of correlation were Bonferroni adjusted for multiple comparisons.

Results

Mesenchymal marker expression on unpassaged bone marrow and passaged BM and HFF-derived MSC.

Bone marrow mononuclear cells obtained from cadaveric vertebrae (16) were serially passaged and harvested for multicolor analysis of mesenchymal marker expression (Figure 1). In unpassaged bone marrow (Figure 1A), CD45−/CD34−/CD31−/CD4−/CD73+/CD105+ (17) mesenchymal stromal cells comprised 0.08% of BM mononuclear cells, 19.4% of which coexpressed CD90. By passage 2 (Figure 1B) CD90+ MSC comprised 83.8% of total mononuclear cells and 96.8% of the CD45−/CD34−/CD31−/CD4− population. For comparison, identical analytical regions were used for analysis of passages 3–10. CD73 expression was consistent between passages, but CD105 was downregulated as a function of passage, with only 54.1% of CD45−/CD34−/CD31−/CD4− cells expressing CD105 at levels consistent with passage 2. There was also a suggestion that CCD73+/CD105+ MSC split into CD90high and CD90low populations at passages 7 and 10. The three independent foreskin fibroblast primary cultures, analyzed at passage 2 (Figure 1C), were consistent with passage 2 BM MSC with respect to CD73, CD105 and CD90 expression. RT-qPCR performed on *CD73* and *CD105* mRNA (Figure 1D, E) did not mirror the quantitative changes observed in cell surface protein expression with passage.

Cell-surface proteomic profiling of unpassaged and passaged mesenchymal stromal cells.

Using the BD 3-Color FACSCap Lyoplate system in combination with a backbone panel, we gated on CD45−/CD14/−CD34−/CD73+/CD105+ cells (Figure S2). Markers that were highly expressed (>70%) in unpassaged bone marrow and p2 HFF, and remained highly expressed in BM MSC during passage included: CD9, CD13, CD29, CD49e, CD73, CD81, CD140b, CD147, and CD151. Markers that modulated during passage are shown in Figure 2. These markers were also tested for statistical correlation with passage number and mRNA expression indicative of senescence (*CDKN2A*), adipogenic (*PPARG*) and osteogenic (*RUNX2*) differentiation (Table 1). In general, markers on p2 HFF tracked with BM MSC, but more detailed analysis (Table S2) revealed a broader array of surface markers in HFF. In BM MSC, modulated cell surface proteins associated with cell death included CD95/Fas, which was upregulated with passage, and CD205/Ly75 and CD273/PD-L2, which were down-regulated with passage. MAC-inhibitory protein/CD59 decreased and MHC Class I increased with passage, the amino acid transporter CD98 upregulated rapidly in culture, while constitutive expression of the multi-drug resistance transporter CD243/P-gp was lost with passage. Passage also resulted in changes to the set of expressed adhesion molecules,

with CD49a, CD49c, CD164/endolyn and CD166/ALCAM increasing with passage, and CD24, CD54/ICAM-1 and CD106/VCAM1 decreasing with passage. Finally, proliferation-associated CD71/transferrin receptor decreased with passage, while motility-associated proteins CD10 and CD63/LAMP3, increased initially and then decreased with passage. Apart from CD71, marker expression on passage 2 HFF was consistent with that of passage 2 BM. The complete list of marker expression by passage is given in Table S2.

Adipogenic and osteogenic differentiation of mesenchymal stromal cells.

PPARG mRNA expression and Oil Red O uptake was monitored for detection of adipogenesis. The product of the *PPARG* gene is a nuclear hormone receptor that is highly expressed in adipocytes (18) and macrophages (19). Ligand-activated PPAR-γ recruits a coactivator which in a complex with retinoid X-receptor binds to DNA leading to transcription of adipogenic genes (20). After 7 days of differentiation in adipogenic medium, RT-qPCR showed that *PPARG* mRNA is highly expressed in MSC of passage 2 but it rapidly decreases with the increasing passage number (Figure 3A). The passage 2 BM MSC cultured in adipogenic medium displayed approximately 6-fold greater values of *PPARG* mRNA than passage 2 cells cultured in control medium. These values decreased at passage 7 and 10 (5- and 4-fold greater values than control cells, respectively). A similar trend was seen microscopically, when lipid vesicles were visualized by Oil Red O staining after 21 days of culture Figure 3B, C). The ability of MSC to differentiate decreased with the increasing passage number. In fact, 18 and 17 % of the cells differentiated at passage 2 and 3, respectively. However, only 9% of MSC were able to differentiate at passage 3 and this ability further decreased to 4% and 2% at passages 7 and 10, respectively (Figure 3C).

Cells were also cultured in the presence of osteogenic medium to further confirm the differentiation capacity of the cultured mesenchymal cells. RT-qPCR of the early osteogenic marker, *RUNX2*, showed that robust early osteogenesis was detected after 7 days of stimulation in passage 2 BM MSCs, but decreased progressively in later passages (Figure 3D). Calcium deposition associated with osteogenesis was measured after 21 days in culture by Alizarin Red staining (Figure 3 E, F). Consistent with *RUNX2* mRNA expression, calcium deposition was greatest in passage 2 and 3 BM MSC and decreased progressively with passage. The low adipogenic and osteogenic differentiation capability of late-passage BM MSC is consistent with the detection of markedly increased *CDKN2A* (*p16)* mRNA, a marker of senescence, in the passages 7 and 10 (Figure 4).

Discussion

One of the major variables in large scale MSC production is the number of passages required to produce a uniform therapeutic product of sufficient cell number to permit large scale clinical trials or to market as a licensed drug. A dose for a 70-kg patient may require as many as 350 million cells (21). Several authors have noted the effects of MSC confluence, passage and mitotic index on phenotype and activity. Ren found that confluent MSC have compromised pro-angiogenic properties and recommended monitoring lactate and glucose levels to estimate confluence and ensure consistency in passage and harvest timing (22). Using a rat model, Crisostomo found that the cardioprotective effects of culture-expanded

murine MSC decrease with passage number and was lost by passage 5 (23). Similarly, Janicki demonstrated that the osteogenic potential of human MSC requires a high proliferative rate and an open chromatin status (24). Characterization and standardization of therapeutic MSC products is an active focus of the Food and Drug Agency in the U.S. (25) and of the Paul-Ehrlich-Institut in Germany (26).

Using a high-throughput cell surface proteomic approach, we characterized the phenotypic profile of unpassaged bone marrow MSC and determined the changes in cell surface markers accompanying passage. The format of the FACSCAP Lyoplate, which features 3 directly conjugated antibodies per well, permitted us to use a multicolor backbone panel to identify and characterize the rare (0.08%, Figure 1) MSC population among a very heterogeneous mixture of bone marrow mononuclear cells. This is the first time, to our knowledge that native BM MSC have been so rigorously profiled. We found that several functional classes of proteins were affected by passage including those influencing cell death, immune regulation, membrane transport, cell adhesion, motility and proliferation (Figure 2). These changes in cell surface marker expression likely reflect changes in function. For example, we show that the adhesion molecule CD106/VCAM1, which is highly expressed in unpassaged MSC, decreases rapidly with culture (Figure 2). The CD106+ subpopulation of MSC has been shown to be more effective in modulating T-helper subsets (27) and has increased potential for vasculogenesis (28). However, loss of CD106 expression *in vitro* can be remedied by exposure to TNF (29). Similarly, we report high expression of CD178/FasL on unpassaged but not cultured MSC. CD178/FasL+, CD273/PD-L2+ MSC may be more potent in inducing the death of CD95/Fas+ or CD279/PD-1+ T cells. Fas signaling triggers a release of TGFβ from macrophages leading to immunotolerance by induction of regulatory T cells (30). We found high expression of FasL in fresh MSCs, however, FasL was rapidly lost with passage (Figure 2). Absence of FasL on cultured MSC has been reported by others (31). It has been shown that co-culture of MSC with the T-cell leukemia cell line Jurkat cell rescues the expression of FasL on MSC (32).

On the other hand, low CD95/Fas expression (Figure 2) or resistance to the Fas pathway (32) is needed for MSC to evade autocrine or T-cell mediated apoptosis. Expression of both Fas and FasL have been previously described in cultured BM MSC (32). Here we show that unpassaged BM MSC do not express Fas, and have high expression of FasL. Nonetheless, even cultured Fas-expressing MSCs have been shown to be resistant to FasL-induced apoptosis, probably at the level of DISC formation (32), allowing them to resist autocrine- or T-cell-mediated apoptosis.

PD-L2 binds to an inhibitory immune receptor PD-1, which is expressed on activated T cells and B cells, macrophages and NK cells (33–36). Engagement of PD-1 results in decreased T-cell proliferation and cytokine production, or cell death by apoptosis. PD-L2 expression has been most widely studied on inflammatory macrophages (37), but has also been detected in human placental MSC. Loss of PDL-2 increases cell adhesion but decreases migration of human placental MSC (38). Interestingly, PDL-2 expression was correlated with both adipogenic and osteogenic capacity (Table 1).

Migration is essential to MSC function in nature, and when administered as a therapeutic. When administered intravenously, MSC must migrate through the endothelial barrier of blood vessels to reach a target tissue. MSC have been shown to express adhesion molecules for cell trafficking (39) and proteases (40,41) involved in MSC migration and adhesion. CD10/neprilysin, a metalloprotease associated with cell motility, was rapidly upregulated in culture, but decreased with early senescence.

Another requirement for therapeutic application of allogeneic MSC is low expression of MHC molecules. Allogeneic cells expressing foreign MHC molecules are rapidly targeted and eliminated by the immune system. We found that MHC class I and class II molecules are minimally expressed on BM MSC *in vivo*, but progressively upregulated with culture. CD59, which prevents formation of the complement membrane attack complex (42), is downregulated with passage.

Transporter expression was also affected by passage. The amino acid transporter CD98/LAT1 was low in in unpassaged MSC and increased rapidly with culture, whereas the stem-cell associated multiple drug resistance transporter CD243/P-glycoprotein was constitutively expressed in 20% of unpassaged BM MSC, and decreased with passage.

When we examined individual markers for statistical correlation with passage number and mRNA expression indicative of senescence, adipogenesis and osteogenesis, only the strongest correlations reached statistical significance, owing to small sample size and correction for multiple comparisons. Loss of MAC-inhibitory protein/CD59, loss of ICAM-1/CD54, and increase in *CDKN2A* with passage, as well as gain of CD10 with adipogenic and osteogenic capacity, were among the strongest associations detected (Table 1).

Three previous reports used conventional HPLC-based proteomics to determine the cell surface proteome cultured BM MSC (43–45). None reported on unpassaged MSC because this would have required sorting approximately 10 million of these rare cells from bone marrow. The advantage of HPLC is that these investigators reported the ability to detect between 463 and 888 cell surface proteins, whereas our panel covered only 228. The disadvantage, compared to flow cytometry is that assessment was semi-quantitative at best, and yielded average expression of all cells in the preparation. Our results agreed with those of Foster *et al.*, with the exception of CD99 and EGFR (both negative in our study), and with those of Jeong *et al.*, with the exception of CD26 (negative in our study). It should be noted that this was not due to sample preparation (trypsinization of adherent cells), since HFF were positive for EGFR and CD26 in our study. Interestingly, we failed to confirm two proteins reported as novel mesenchymal markers by Niehage (CD97 and CD112).

Taken together, our data suggest a panel of several markers associated with robust MSC function. The most prominent changes associated with early senescence and an accompanying lack of differentiation capacity were loss of CD10 (motility) and CD71 (proliferation) (Figure 2) and increase in *p16* (Figure 4).

Cell passage number is a surrogate for the number of cell-doublings, which is the critical factor determining when cell cultures become senescent. In the 1960s Hayflick used the

term senescence to describe the failure of human diploid cell cultures after multiple passages (46). He noted that human fetal lung cultures stopped growing and then died at approximately passage 50. In the present study, we detected increased levels of *CDKN2A*/*p16* mRNA, a marker of senescence (47), by passage 7. This correlated with, or was preceded by numerous cell surface changes described above. Perhaps the only way to produce the large-scale cell banks required for cellular therapy while minimizing the number of cell-doublings is to start with a large number of unpassaged MSC. This could be accomplished several ways, including pooling cells isolated from an alternative source, such as placenta (48), or using an MSC-rich tissue like adipose, that can be harvested in bulk from living donors (49). Our preferred solution is to isolate bone marrow MSC from cadaveric bone. This is an underused resource that is available from heart-beating organ donors. We have described a GMP-compliant method for isolation of large numbers on bone marrow mononuclear cells ($3.9 \pm 0.7 \times 10^{10}$) from 8 harvested vertebrae (Th8-L4) (14,50). This is greater than 100-fold more cells than can be isolated from 15 mL bone marrow aspirated from a living donor. We have used unpassaged cadaveric bone marrow cells in two clinical trials (50,51), and have performed proof of principal experiments demonstrating that they are an excellent source of cultured MSC.

Supplementary Material

Refer to Web version on PubMed Central for supplementary material.

Acknowledgements.

This work was funded by grants BC032981, BC044784, W81XWH-12–1-0415 and BC132245_W81XWH-14–0258 from the Department of Defense, National Cancer Institute grant R21 CA191647 and RO1-CA114246, the Commonwealth of Pennsylvania, the Hillman Foundation and the Glimmer of Hope Foundation. The UPCI Cytometry, Cell Culture and Cytogenetics, and Biostatistics Facilities are supported by CCSG P30CA047904.

ClinicalTrials.gov Identifier: NCT01852370. National Institutes of Health; 2018.

The authors would like Mr. Bosko Popov for his excellent technical assistance, Dr. Daniel P. Normolle for his statistical expertise, and Suraj Saksena and Christian Carson of BD Biosciences for providing the BD BDT FACSCAP Lyoplate™ Human Cell Surface Marker Screening Panel.

References

1. Fuchs E, Segre JA. Stem cells: a new lease on life. Cell 2000;100:143–55. [PubMed: 10647939]
2. Wu Y, Chen L, Scott Paul G, Tredget Edward E. Mesenchymal Stem Cells Enhance Wound Healing Through Differentiation and Angiogenesis. STEM CELLS 2009;25:2648–2659.
3. Cooper K, Viswanathan C. Establishment of a mesenchymal stem cell bank. Stem Cells Int 2011;2011:1–8.
4. Bustos ML, Huleihel L, Meyer EM, Donnenberg AD, Donnenberg VS, Sciurba JD, Mroz L, McVerry BJ, Ellis BM, Kaminski N and others. Overexpression of IL-10 and IL-1RN by activated human mesenchymal stem cells improves their therapeutic effect in lung injury. Stem Cells Translational Medicine 2013;In Press.
5. Singer NG, Caplan AI. Mesenchymal stem cells: mechanisms of inflammation. Annu Rev Pathol 2011;6:457–78. [PubMed: 21073342]
6. Prockop DJ, Youn Oh J. Mesenchymal Stem/Stromal Cells (MSCs): Role as Guardians of Inflammation. Mol Ther 2012;20:14–20. [PubMed: 22008910]

7. Strassmann G, Patil-Koota V, Finkelman F, Fong M, Kambayashi T. Evidence for the involvement of interleukin 10 in the differential deactivation of murine peritoneal macrophages by prostaglandin E2. The Journal of Experimental Medicine 1994;180:2365–2370. [PubMed: 7525853]
8. Ivanova-Todorova E, Bochev I, Mourdjeva M, Dimitrov R, Bukarev D, Kyurkchiev S, Tivchev P, Altunkova I, Kyurkchiev DS. Adipose tissue-derived mesenchymal stem cells are more potent suppressors of dendritic cells differentiation compared to bone marrow-derived mesenchymal stem cells. Immunology Letters 2009;126:37–42. [PubMed: 19647021]
9. Peng W, Gao T, Yang Z-l, Zhang S-c, Ren M-l, Wang Z-g, Zhang B. Adipose-derived stem cells induced dendritic cells undergo tolerance and inhibit Th1 polarization. Cellular Immunology 2012;278:152–157. [PubMed: 22982671]
10. Silva M, Donnenberg VS, Rubin JP, Zimmerlin L, Donnenberg AD. Antiinflammatory Stem Cell Principles In: Coleman S, Mazzola R, Pu L, editors. Fat Injection: From Filling to Regeneration Second ed. Volume In Press: CRC Press, Taylor and Francis Group; 2017.
11. Lalu MM, McIntyre L, Pugliese C, Fergusson D, Winston BW, Marshall JC, Granton J, Stewart DJ. Safety of Cell Therapy with Mesenchymal Stromal Cells (SafeCell): A Systematic Review and Meta-Analysis of Clinical Trials. PLOS ONE 2012;7:e47559. [PubMed: 23133515]
12. Zhao Q, Ren H, Han Z. Mesenchymal stem cells: Immunomodulatory capability and clinical potential in immune diseases. Journal of Cellular Immunotherapy 2016;2:3–20.
13. Crisan M, Yap S, Casteilla L, Chen CW, Corselli M, Park TS, Andriolo G, Sun B, Zheng B, Zhang L and others. A perivascular origin for mesenchymal stem cells in multiple human organs. Cell stem cell 2008;3:301–13. [PubMed: 18786417]
14. Gorantla VS, Schneeberger S, Moore LR, Donnenberg VS, Zimmerlin L, Lee WPA, Donnenberg AD. Development and Validation of a Procedure to Isolate Viable Bone Marrow Cells from the Vertebrae of Cadaveric Organ Donors for Composite Organ Grafting Vertebrae of Cadaveric Organ Donors for Composite Organ Grafting. Cytotherapy 2012;14:104–113. [PubMed: 21905958]
15. Biedermann KA, Landolph JR. Induction of Anchorage Independence in Human Diploid Foreskin Fibroblasts by Carcinogenic Metal Salts. Cancer Research 1987;47:3815. [PubMed: 3594439]
16. Gorantla VS, Schneeberger S, Moore LR, Donnenberg VS, Zimmerlin L, Lee WP, Donnenberg AD. Development and validation of a procedure to isolate viable bone marrow cells from the vertebrae of cadaveric organ donors for composite organ grafting. Cytotherapy 2012;14:104–13. [PubMed: 21905958]
17. Dominici M, Le Blanc K, Mueller I, Slaper-Cortenbach I, Marini F, Krause D, Deans R, Keating A, Prockop D, Horwitz E. Minimal criteria for defining multipotent mesenchymal stromal cells. The International Society for Cellular Therapy position statement. Cytotherapy 2006;8:315–7. [PubMed: 16923606]
18. Chawla A, Schwarz EJ, Dimaculangan DD, Lazar MA. Peroxisome proliferator-activated receptor (PPAR) gamma: adipose-predominant expression and induction early in adipocyte differentiation. Endocrinology 1994;135:798–800. [PubMed: 8033830]
19. Tontonoz P, Nagy L, Alvarez JG, Thomazy VA, Evans RM. PPARgamma promotes monocyte/macrophage differentiation and uptake of oxidized LDL. Cell 1998;93:241–52. [PubMed: 9568716]
20. Nolte RT, Wisely GB, Westin S, Cobb JE, Lambert MH, Kurokawa R, Rosenfeld MG, Willson TM, Glass CK, Milburn MV. Ligand binding and co-activator assembly of the peroxisome proliferator-activated receptor-gamma. Nature 1998;395:137–43. [PubMed: 9744270]
21. Hare JM, Traverse JH, Henry TD, Dib N, Strumpf RK, Schulman SP, Gerstenblith G, DeMaria AN, Denktas AE, Gammon RS and others. A Randomized, Double-Blind, Placebo-Controlled, Dose-Escalation Study of Intravenous Adult Human Mesenchymal Stem Cells (Prochymal) After Acute Myocardial Infarction. Journal of the American College of Cardiology 2009;54:2277–2286. [PubMed: 19958962]
22. Ren J, Wang H, Tran K, Civini S, Jin P, Castiello L, Feng J, Kuznetsov SA, Robey PG, Sabatino M and others. Human bone marrow stromal cell confluence: effects on cell characteristics and methods of assessment. Cytotherapy 2015;17:897–911. [PubMed: 25882666]

23. Crisostomo PR, Wang M, Wairiuko GM, Morrell ED, Terrell AM, Seshadri P, Nam UH, Meldrum DR. High passage number of stem cells adversely affects stem cell activation and myocardial protection. Shock 2006;26:575–80. [PubMed: 17117132]
24. Janicki P, Boeuf S, Steck E, Egermann M, Kasten P, Richter W. Prediction of in vivo bone forming potency of bone marrow-derived human mesenchymal stem cells. Eur Cell Mater 2011;21:488–507. [PubMed: 21710441]
25. Mendicino M, Bailey Alexander M, Wonnacott K, Puri Raj K, Bauer Steven R. MSC-Based Product Characterization for Clinical Trials: An FDA Perspective. Cell Stem Cell 2014;14:141–145. [PubMed: 24506881]
26. Wuchter P, Bieback K, Schrezenmeier H, Bornhäuser M, Müller LP, Bönig H, Wagner W, Meisel R, Pavel P, Tonn T and others. Standardization of Good Manufacturing Practice–compliant production of bone marrow–derived human mesenchymal stromal cells for immunotherapeutic applications. Cytotherapy 2015;17:128–139. [PubMed: 24856898]
27. Yang ZX, Han ZB, Ji YR, Wang YW, Liang L, Chi Y, Yang SG, Li LN, Luo WF, Li JP and others. CD106 identifies a subpopulation of mesenchymal stem cells with unique immunomodulatory properties. PLoS One 2013;8:e59354. [PubMed: 23555021]
28. Lu S, Ge M, Zheng Y, Li J, Feng X, Feng S, Huang J, Feng Y, Yang D, Shi J and others. CD106 is a novel mediator of bone marrow mesenchymal stem cells via NF-kappaB in the bone marrow failure of acquired aplastic anemia. Stem Cell Res Ther 2017;8:178. [PubMed: 28764810]
29. Halfon S, Abramov N, Grinblat B, Ginis I. Markers distinguishing mesenchymal stem cells from fibroblasts are downregulated with passaging. Stem Cells Dev 2011;20:53–66. [PubMed: 20528146]
30. Akiyama K, Chen C, Wang D, Xu X, Qu C, Yamaza T, Cai T, Chen W, Sun L, Shi S. Mesenchymal-stem-cell-induced immunoregulation involves FAS-ligand-/FAS-mediated T cell apoptosis. Cell Stem Cell 2012;10:544–55. [PubMed: 22542159]
31. Ryan JM, Barry FP, Murphy JM, Mahon BP. Mesenchymal stem cells avoid allogeneic rejection. J Inflamm (Lond) 2005;2:8. [PubMed: 16045800]
32. Mazar J, Thomas M, Bezrukov L, Chanturia A, Pekkurnaz G, Yin S, Kuznetsov SA, Robey PG, Zimmerberg J. Cytotoxicity mediated by the Fas ligand (FasL)-activated apoptotic pathway in stem cells. J Biol Chem 2009;284:22022–8. [PubMed: 19531476]
33. Roy S, Gupta P, Palit S, Basu M, Ukil A, Das PK. The role of PD-1 in regulation of macrophage apoptosis and its subversion by Leishmania donovani. Clin Transl Immunology 2017;6:e137. [PubMed: 28690843]
34. Nishimura H, Agata Y, Kawasaki A, Sato M, Imamura S, Minato N, Yagita H, Nakano T, Honjo T. Developmentally regulated expression of the PD-1 protein on the surface of double-negative (CD4-CD8-) thymocytes. Int Immunol 1996;8:773–80. [PubMed: 8671666]
35. Thibult ML, Mamessier E, Gertner-Dardenne J, Pastor S, Just-Landi S, Xerri L, Chetaille B, Olive D. PD-1 is a novel regulator of human B-cell activation. Int Immunol 2013;25:129–37. [PubMed: 23087177]
36. Liu Y, Cheng Y, Xu Y, Wang Z, Du X, Li C, Peng J, Gao L, Liang X, Ma C. Increased expression of programmed cell death protein 1 on NK cells inhibits NK-cell-mediated anti-tumor function and indicates poor prognosis in digestive cancers. Oncogene 2017;36:6143–6153. [PubMed: 28692048]
37. Pn Loke, Allison JP. PD-L1 and PD-L2 are differentially regulated by Th1 and Th2 cells. Proceedings of the National Academy of Sciences 2003;100:5336–5341.
38. Wang G, Zhang S, Wang F, Li G, Zhang L, Luan X. Expression and biological function of programmed death ligands in human placenta mesenchymal stem cells. Cell Biol Int 2013;37:137–48. [PubMed: 23319413]
39. Zhu H, Mitsuhashi N, Klein A, Barsky Lora W, Weinberg K, Barr Mark L, Demetriou A, Wu Gordon D. The Role of the Hyaluronan Receptor CD44 in Mesenchymal Stem Cell Migration in the Extracellular Matrix. STEM CELLS 2009;24:928–935.
40. De Becker A, Van Hummelen P, Bakkus M, Vande Broek I, De Wever J, De Waele M, Van Riet I. Migration of culture-expanded human mesenchymal stem cells through bone marrow endothelium

is regulated by matrix metalloproteinase-2 and tissue inhibitor of metalloproteinase-3. Haematologica 2007;92:440–449. [PubMed: 17488654]

41. Ponte AL, Marais E, Gallay N, Langonné A, Delorme B, Hérault O, Charbord P, Domenech J. The In Vitro Migration Capacity of Human Bone Marrow Mesenchymal Stem Cells: Comparison of Chemokine and Growth Factor Chemotactic Activities. STEM CELLS 2007;25:1737–1745. [PubMed: 17395768]
42. Farkas I, Baranyi L, Ishikawa Y, Okada N, Bohata C, Budai D, Fukuda A, Imai M, Okada H. CD59 blocks not only the insertion of C9 into MAC but inhibits ion channel formation by homologous C5b-8 as well as C5b-9. The Journal of Physiology 2002;539:537–545. [PubMed: 11882685]
43. Niehage C, Steenblock C, Pursche T, Bornhäuser M, Corbeil D, Hoflack B. The Cell Surface Proteome of Human Mesenchymal Stromal Cells. PLoS ONE 2011;6:e20399. [PubMed: 21637820]
44. Jeong JA, Ko KM, Park HS, Lee J, Jang C, Jeon CJ, Koh GY, Kim H. Membrane proteomic analysis of human mesenchymal stromal cells during adipogenesis. Proteomics 2007;7:4181–91. [PubMed: 17994623]
45. Foster LJ, Zeemann PA, Li C, Mann M, Jensen ON, Kassem M. Differential expression profiling of membrane proteins by quantitative proteomics in a human mesenchymal stem cell line undergoing osteoblast differentiation. Stem Cells 2005;23:1367–77. [PubMed: 16210410]
46. Hayflick L The limited in vitro lifetime of human diploid cell strains. Experimental Cell Research 1965;37:614–636. [PubMed: 14315085]
47. Alcorta DA, Xiong Y, Phelps D, Hannon G, Beach D, Barrett JC. Involvement of the cyclin-dependent kinase inhibitor p16 (INK4a) in replicative senescence of normal human fibroblasts. Proceedings of the National Academy of Sciences of the United States of America 1996;93:13742–13747. [PubMed: 8943005]
48. Talwadekar MD, Kale VP, Limaye LS. Placenta-derived mesenchymal stem cells possess better immunoregulatory properties compared to their cord-derived counterparts–a paired sample study. Scientific Reports 2015;5:15784. [PubMed: 26507009]
49. Zimmerlin L, Donnenberg VS, Rubin JP, Donnenberg AD. Mesenchymal markers on human adipose stem/progenitor cells. Cytometry Part A 2013;83A:134–140.
50. Donnenberg AD, Gorantla VS, Schneeberger S, Moore LR, Brandacher G, Stanczak HM, Koch EK, Lee WPA. Clinical implementation of a procedure to prepare bone marrow cells from cadaveric vertebral bodies. Regenerative Medicine 2011;6:701–706. [PubMed: 22050522]
51. Sequential Cadaveric Lung and Bone Marrow Transplant for Immune Deficiency Diseases (BOLT +BMT),

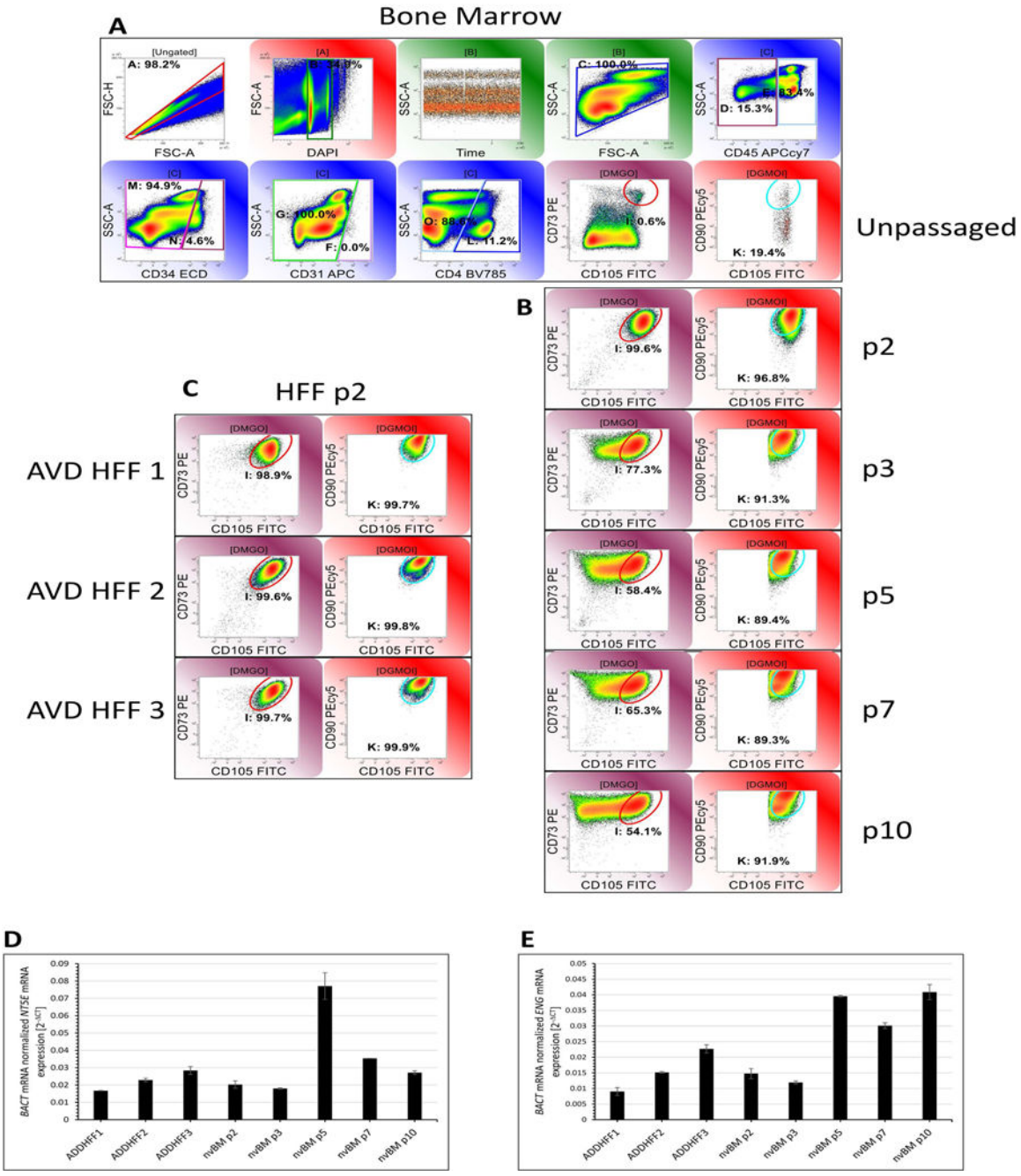

Figure 1. Mesenchymal marker expression on unpassaged bone marrow and passaged BM and HFF-derived MSC.

A: Unpassaged bone marrow mononuclear cells (Gate C: 2,309,684 clean events were acquired,). Mesenchymal markers CD73 and CD105 were measured after doublet discrimination on forward scatter area and height, selection for events with 2N-4N DNA content and light scatter consistent with bone marrow cells and elimination of cells expressing CD45, CD34, CD31 and CD4. The identical gating strategy was used for panels B and C (not shown). CD90 was measured on CD73/CD105+ events. MSC constituted 0.6% of the gated population and 0.08% of BM mononuclear cells, 19.4% of which were CD90+.

B: Serial passages of adherent bone marrow mononuclear cells. C: Three independent human foreskin fibroblast isolates. All HFF samples were assayed at passage 2. D and E: RT-qPCR was used to confirm mRNA for mesenchymal markers *NT5E* (*CD73)* and *ENG* (*CD105)*. *BACT* was used as a normalizing housekeeping gene. Data represent mean ± SEM from three independent experiments.

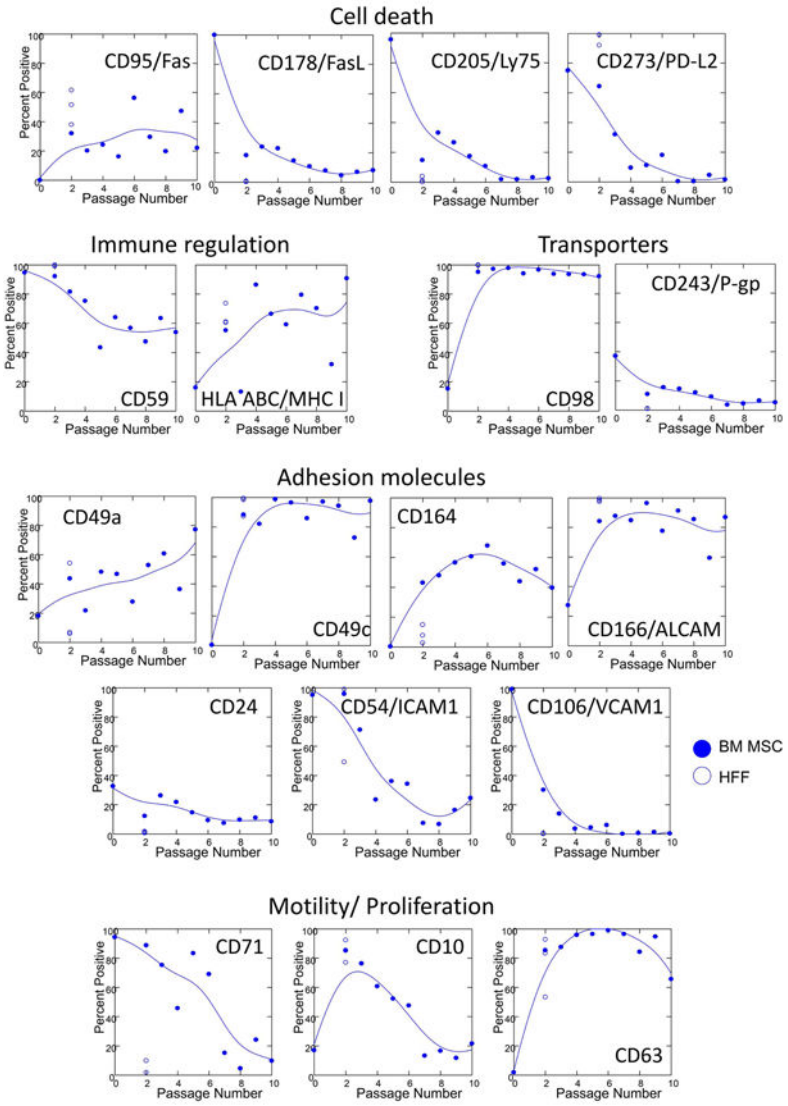

Figure 2. Markers which were highly modulated during MSC passage.

Cell surface proteomics was performed on unpassaged bone marrow and on cultured MSC (passages 2–10). Markers of cell death, immune regulation, transporters, adhesion molecules, and motility and proliferation, which changed as a function of passage are shown. A complete list of 228 markers is provided in Table S2. Results from HFF harvested at p2 (open circles) are shown for comparison. Curves were fit to MSC data using the method of distance weighted least squares as implemented by SYSTAT statistical software

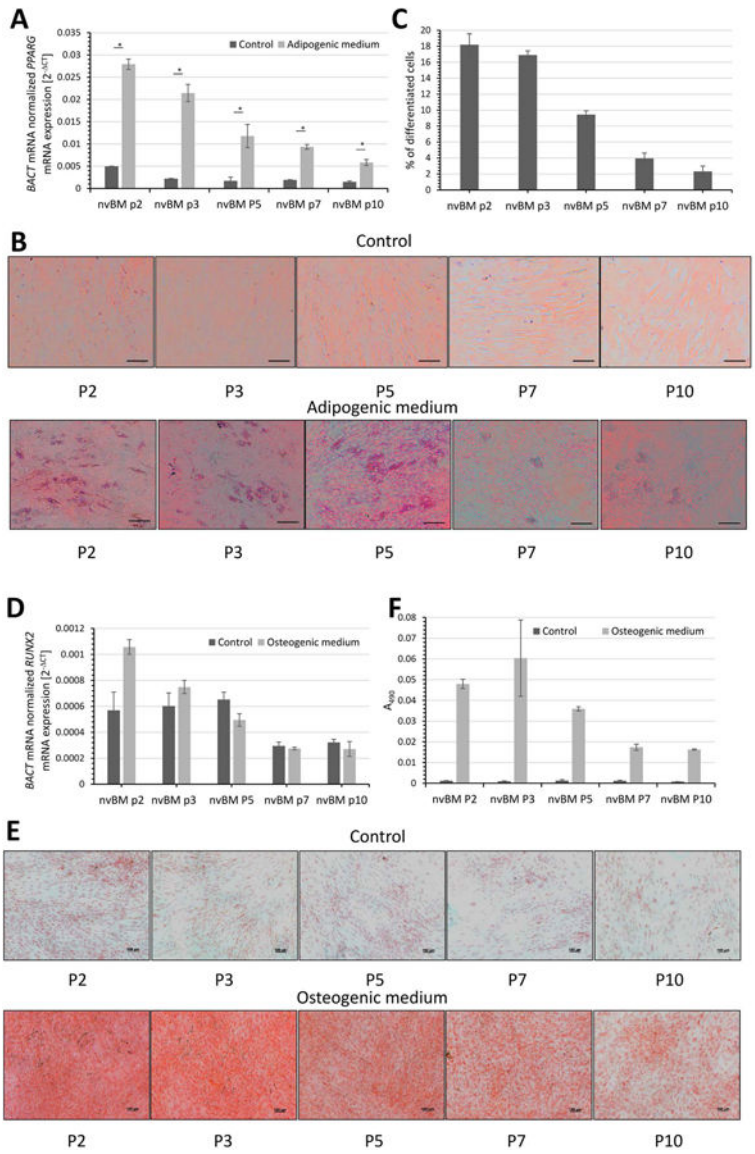

Figure 3. Adipogenesis and Osteogenesis of cultured bone marrow-derived human mesenchymal cells.

A-C: Human bone marrow cells were isolated as described in Materials and Methods. Adherent mesenchymal cells were cultured in control, adipogenic or osteogenic medium. A) RT-qPCR of *PPARG* mRNA adipogenesis marker after 7 days of differentiation. Data represent mean ± SEM from three independent experiments. Asterisks indicate *P* value <0.05 (Student's paired t-test, two-tailed). B) Oil red O staining of cultured control and differentiated cells after 21 days is shown. The scale bar indicates 100 μm. C) Quantification of adipocytes after 21 days in adipogenic differentiation medium. Data represent mean ± SEM from 4 fields (10x objective) of two independent experiments. D-F: This experiment was performed in parallel to the experiment reported in panels A-C. Adherent mesenchymal cells were cultured in control or osteogenic medium. D) RT-qPCR of *RUNX2* mRNA a marker of early osteogenesis was measured after 7 days of treatment. Data represent mean ± SEM from three independent experiments. E) Alizarin red staining of cultured control and

osteogenic-differentiated cells after 21 days is shown. The scale bar indicates 100 μm. F) Quantitative analysis of the extracted Alizarin Red in 20% methanol and 10% acetic acid. The absorption of the dissolved dye was read on the spectrophotometer at 490 nm. Data represent mean ± SEM from two independent experiments.

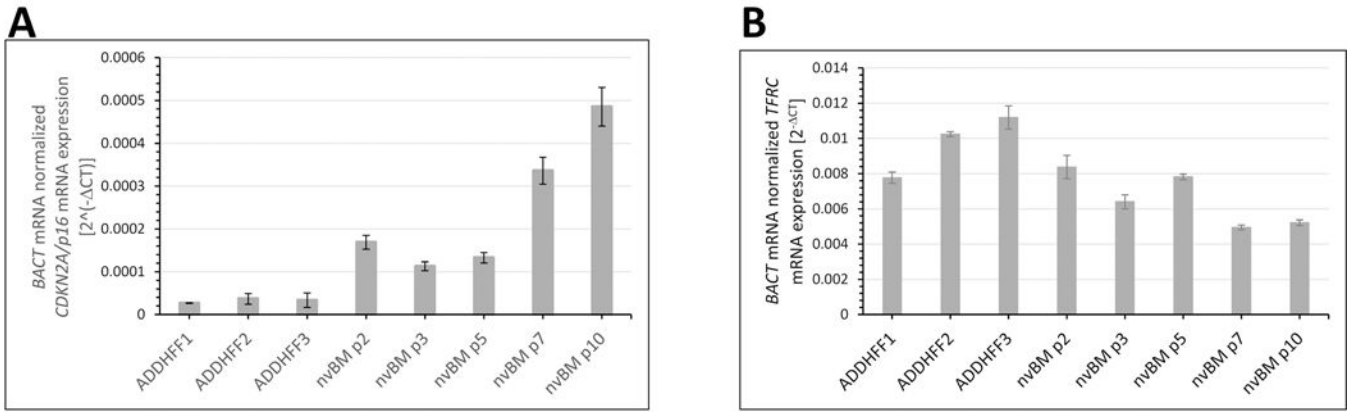

Figure 4. Senescence and proliferation of cultured MSC.

A) *CDKN2A* (p16) , a senescence marker and B) *TFRC* (CD71), a marker of proliferation were measured by RT-qPCR to detect changes occurring in BM-derived MSC between passages 2 and 10. *BACT* was used as a normalizing housekeeping gene. Data represent mean ± SEM from three independent experiments. *CDKN2A* expression was highly correlated with passage number in cultured MSC (Pearson's coefficient of correlation $R = 0.942$, $p < 0.001$), but *TRFC* expression was uncorrelated ($R = 0.261$, $p > 0.9$).

Table 1.

Correlation of selected proteins with passage number, the senescence marker *CDKN2A* (p16), the adipogenesis marker *PPARG* or the osteogenesis marker *RUNX2*.

Markers are those shown in Figure 2 that correlate with at least one mRNA outcome or passage number. Negative R values indicate an inverse correlation. Pearson coefficients of correlation (R) and Bonferroni corrected p-values (p) are shown. N.S. = not significant, p>0.05.

				Senescence		Adipose		Osteo	
Reagent	**Function**	**Passage Number**		***CDKN2A***		***PPARG***		***RUNX2***	
		R	**p**	**R**	**p**	**R**	**p**	**R**	**p**
PDL2	Cell death	−0.369	N.S.	−0.802	N.S.	**0.971**	**0.017**	**0.988**	**0.005**
CD59	Negative Immune Reg	**−0.885**	**<0.001**	−0.705	N.S.	0.904	N.S.	0.860	N.S.
CD98	Transporter	**0.649**	**0.011**	**−0.879**	**0.012**	0.764	N.S.	0.686	N.S.
CD49a	Adhesion	**0.768**	**0.001**	0.753	N.S.	−0.710	N.S.	−0.631	N.S.
CD49c	Adhesion	**0.690**	**0.005**	0.246	N.S.	−0.824	N.S.	−0.769	N.S.
CD54	Adhesion	**−0.711**	**0.003**	−0.701	N.S.	**0.953**	**0.037**	**0.981**	**0.01**
CD106	Adhesion	−0.288	N.S.	−0.065	N.S.	**0.966**	**0.022**	**0.982**	**0.008**
CD10	Motility	**−0.598**	**0.026**	**−0.879**	**0.012**	0.928	N.S.	**0.954**	**0.035**
CDKN2A	Senescence	**0.942**	**0.001**						
PPARG	Adipose	−0.931	N.S.						
RUNX2	Osteo	−0.905	N.S.						